Clinical and Experimental Immunology, 2022, **207**, 360–369
https://doi.org/10.1093/cei/uxac004
Advance access publication 28 January 2022
Research Article

Clinical & Experimental IMMUNOLOGY

OXFORD

Research Article

Interleukin 17 receptor E identifies heterogeneous T helper 17 cells in peritoneal fluid of moderate and severe endometriosis patients

Yanping Jiang[1,*,‡], Lu Wang[1,‡], Yaqin Peng[1], Jian Qin[2], Aili Tan[1], and Shujun Wang[1]

[1]Department of Gynaecology, Renmin Hospital of Wuhan University, Wuhan, Hubei, PR China
[2]Renmin Hospital of Wuhan University, Wuhan, Hubei, PR China

*Correspondence: Yanping Jiang, Department of Gynaecology, Renmin Hospital of Wuhan University, Wuhan, Hubei, PR China. E-mail: jiang_yanping@whu.edu.cn
‡Yanping Jiang and Lu Wang contributed equally to this study.

Abstract

Endometriosis is a chronic inflammatory disorder resulting in pelvic pain and infertility. The role of T helper 17 (Th17) cells in endometriosis remains elusive. In this study, through detecting CXCR3, CCR4, CCR10, CCR6, interleukin-17 Receptor E (IL-17RE), and CD27, RORγt-and-IL-17A-expressing Th17 cells were distinguished and sorted from peritoneal fluid (PF) of patients with stage III and IV endometriosis. Furthermore, we found that IL-17RE and CD27 were the labels of heterogeneous PF Th17 subsets, i.e. IL-17RE^{-}CD27^{-} subset, IL-17RE^{+}CD27^{-} subset, and IL-17RE^{+}CD27^{+} subset. The former two subsets expressed higher IL-17A, GM-CSF, and IL-22 and were more proliferative than the latter subset. RNA-Seq analysis on IL-17RE^{+} Th17 subset and IL-17RE^{-} Th17 subset revealed up-regulation of genes involved in oxidative phosphorylation and electron transport chain in IL-17RE^{+} Th17 subset relative to IL-17RE^{-} Th17 subset. Consistently, the IL-17RE^{+} Th17 subset produced more adenosine triphosphate (ATP) and reactive oxygen species (ROS) than IL-17RE^{-} Th17 subset. In conclusion, this study provides a novel method to detect and isolate live PF Th17 cells from endometriosis patients and unveils the functional and metabolic heterogeneity of PF Th17 subsets. Therefore, it sheds light on the elucidation of molecular mechanisms that modulate the function of pathological Th17 cells in endometriosis.

Keywords: endometriosis, T helper 17 (Th17) cells, interleukin 17 receptor E, CD27, oxidative phosphorylation, electron transport chain

Abbreviations: Th17, T helper 17;IL-17RE, Interleukin 17 receptor E; PF, peritoneal fluid;ATP, adenosine triphosphate;ROS, reactive oxygen species; Th2, T helper 2; r-AFS, revised American Fertility Society score; BSA, bovine serum albumin;GO, Gene Ontology; KEGG, Kyoto Encyclopedia of Genes and Genomes; HBSS, Hank's balanced salt solution; H2DCFDA, 2, 7-dichlorodihydrofluorescein diacetate; cpm, counted photons per minute

Introduction

Endometriosis is a chronic inflammatory disorder resulting in pelvic pain and infertility [1]. Various immune cell types, including neutrophils, macrophages, and T cells, play significant roles in the initiation and progression of endometriosis [2]. Immune cells secret biochemical factors that facilitate endometriotic cell division, invasion, as well as angiogenesis [3]. However, the exact functions and regulatory mechanisms of these immune cells have not been thoroughly elucidated.

Previous findings suggest that imbalanced T-cell subsets contribute to inflammatory reactions in endometriosis tissues. Cytokines released by peritoneal T-cells are predominantly T helper 2 (Th2) cytokines in endometriosis tissue [4]. Regulatory T-cell deficiency seems to promote local inflammation, angiogenesis, and facilitate the attachment and growth of endometrial implants [5]. Recent studies have revealed the role of T helper 17 (Th17) cells in endometriosis pathophysiology. Th17 cells produce IL-17A to contribute to the development of inflammatory and autoimmune diseases. The proportion of Th17 cells in endometriosis lesions is higher than that in the normal endometrium [6], and their high proportion in peritoneal fluid (PF) is related to the severity of endometriosis [7]. However, the heterogeneity and plasticity of Th17 cells in patients with endometriosis remain poorly understood. It is, therefore, important to isolate live Th17 cells from blood, lymphoid organs, PF, and endometriosis lesions to characterize their activities. Unfortunately, previous and current studies on human Th17 cells rely on intracellular staining of IL-17A, making the isolation of live Th17 cells impossible. Several research groups used an array of chemokine receptors to dissect T-cell subsets including Th17 cells in other diseases [8–11]. However, whether these receptors apply to Th17 detection in endometriosis remains untested.

In the present study, we use a set of cell surface markers to detect and sort live Th17 cells from PF of patients with moderate/severe endometriosis. Moreover, RNA-Seq analysis revealed significant distinct transcript profiles of PF Th17 subpopulations. Therefore, our data disclose the heterogeneity of PF Th17 cells in endometriosis.

Received 26 July 2021; Revised 26 November 2021; Accepted for publication 25 January 2022

Materials and methods

Patients

This study was approved by the Research Ethics Committee of Renmin Hospital of Wuhan University with written informed consent obtained from all participants. Between April 2018 and November 2020, according to the revised American Fertility Society score (r-AFS), 48 women with stage III–IV endometriosis were recruited at the Department of Gynecology in Renmin Hospital of Wuhan University. The demographic information is presented in Table 1.

Enrichment of mononuclear cells from PF

Under general anesthesia, PF was collected from the pouch of Douglas at the start of laparoscopy. Any blood-containing PF was discarded and not included in the study. PF mononuclear cells were overlaid on the lymphocyte separation medium (Sigma–Aldrich) and enriched by density-gradient centrifugation at 400×*g* for 20 min. Cells in the interface were harvested, washed with PBS, and incubated in 200 µl of red blood cell lysis buffer (Thermo Fisher) for 15 min at room temperature to remove residual red blood cells. The cells were then washed with PBS and suspended in PBS containing 2 mM EDTA and 0.5% bovine serum albumin (BSA) for flow cytometry. In some experiments, venous blood was collected from patients and red blood cells were lysed as described above. Blood leukocytes were suspended in PBS containing 2 mM EDTA and 0.5% BSA for flow cytometry.

Flow cytometry

The following antibodies were used: APC/Cy7 anti-CD3 (HIT3a), FITC anti-CD4 (A161A1), PE anti-CCR4 (L291H4), PE/Cy7 anti-CXCR3 (G025H7), PerCP/Cy5.5 anti-CCR6 (29-2L17), APC anti-CCR10 (6588-5), PE anti-CD14 (63D3), PE anti-CXCR3 (G025H7), PE anti-CCR10 (6588-5), PE/Cy7 anti-CCR4 (L291H4), APC/Cy7 anti-CD27 (M-T271), Pacific blue anti-IL-17A (BL168), and Pacific blue anti-GM-CSF (BVD2-21C11) were purchased from BioLegend. APC anti-IL-17RE (FAB8358A) was purchased from R&D Systems. To stain cell surface markers, PF mononuclear cells were incubated with 2 µg/ml of each antibody for 30 min on ice before analysis and sorting on a BD FACSAria Flow Cytometer (BD Biosciences). To stain intracellular cytokines after surface marker staining, cells were fixed with 200 µl of 2% paraformaldehyde for 20 min, followed by permeabilization in 1 ml of 90% methanol-PBS on ice for 25 min. Cells were then incubated with 5 µg/ml of each antibody for 1 h at room temperature, respectively. Cells were washed and suspended in PBS for analysis on an LSRII flow cytometer with a UV laser (BD Biosciences).

Table 1. Clinical demographic data

Parameters	Stage III ($n = 25$)	Stage IV ($n = 23$)
Age (y)	30.36 ± 2.0	30.30 ± 1.60
BMI	22.62 ± 2.4	22.57 ± 2.29
Menstrual phase (follicular/luteal)	15/10	13/10
Gravidity	1.6 ± 0.98	1.48 ± 0.97
Parity	1.08 ± 0.69	0.82 ± 0.64
Hormonal treatment	5 (20%)	6 (26%)
Peritoneal wash fluid (ml)	37 ± 3.04	36.7 ± 4.46
Endometrioma	4 (16%)	7 (17%)
Superficial endometriosis	21 (84%)	19 (83%)
Deep endometriosis	4 (16%)	7 (17%)

RNA-Seq

PF Th17 cell subpopulations were sorted from 5 patients and pooled for RNA-Seq. Cellular RNA was extracted using the Arcturus PicoPure RNA Isolation Kit (Thermo Fisher). The quality and quantities of RNA samples were measured with the QIAxcel RNA QC Kit v2.0 (Qiagen) following the manufacturer's instructions. One microgram RNA at the concentration >200 ng/µl was subjected to library construction, sequencing, reads quality check, alignment, clustering, expression assessment, Gene Ontology (GO) enrichment analysis, and Kyoto Encyclopedia of Genes and Genomes (KEGG) enrichment analysis by the Wuhan SeqHealth Co., Ltd. The Collibri™ Stranded RNA Library Prep Kit for Illumina (Thermo Fisher), HiSeq 2000 Sequencing System (Illumina), TopHat v2.1.1, HTSeq v0.12.4, DEGseq2, and Hypergeometric test were used for the above procedures, respectively.

Validation of DEGs by quantitative polymerase chain reaction (qPCR)

cDNA preparation was achieved using the PrimeScript 1st strand cDNA Synthesis Kit (Takara Bio). qPCR was implemented using the SYBR Green Quantitative RT-PCR (Sigma–Aldrich) on an Azure Cielo 3 Real-Time qPCR System (Azure Biosystems). The PCR cycle condition was 50°C for 2 min, 95°C for 10 min, 95°C for 15 s and 60°C for 30 s in 40 cycles, then 72°C for10 min. After normalization to β-actin mRNA level, the relative transcript amounts were determined by the $2^{-\Delta\Delta Ct}$ method. The primer sequences are displayed in Table S1.

Cell cycle analysis

Sorted Th17 subpopulations were fixed in ice-cold 70% ethanol for 2.5 h. Cells were centrifuged for 5 min at 300×*g* at 4°C. Ethanol was removed and cells were rinsed with ice-cold Hank's balanced salt solution (HBSS) containing Mg^{2+} and Ca^{2+}. After that, cells were suspended in 0.5 ml of ice-cold HBSS containing Mg^{2+} and Ca^{2+}. The cell suspension was mixed with an equal volume of HBSS containing 2 mg Hoechst 33342 (Molecular Probes) and 4 mg Pyronin Y (Sigma–Aldrich) and incubated for 20 min in the dark. Cells were then loaded on the flow cytometer for cell cycle analysis.

Adenosine triphosphate (ATP) assay

The ATP amount evaluation was conducted using the Luminescent ATP Detection Assay Kit (ab113849, Abcam) following the manufacturer's protocol.

ROS detection

Intracellular reactive oxygen species (ROS) were assessed by 2,7-dichlorodihydrofluorescein diacetate (H2DCFDA) staining. Th17 cells were incubated in pre-warmed PBS containing 10 µM H2DCFDA (Thermo Fisher) for 15 min at 37°C. After two washes with PBS, cells were suspended in PBS and the green fluorescence was measured by flow cytometry.

To measure ROS in PF, aliquots of 400 µl of unprocessed PF were prepared in duplicate, followed by adding 10 µl of

luminol (5 mM in dimethyl sulphoxide, Sigma–Aldrich) to the specimens. Chemiluminescence was recorded for 15 min in the integration mode on a STELLUX® 4400 chemiluminescence plate reader (ALPCO). Results were presented as $\times 10^4$ counted photons per minute (cpm).

Statistics

Each experiment was independently performed 2 or 3 times. The data were shown as mean ± standard deviation unless specified. The Student's *t*-test, non-parametric Mann–Whitney *U* test, or Kruskal–Wallis test was used to compare the data. A *P*-value <0.05 was regarded as significant.

Results

The phenotype of PF IL-17-producing T-cells in endometriosis

Several cell surface markers have been applied to distinguish T-cell subsets [12, 13]. To characterize the phenotype of PF Th17 cells, we first detected the expression of these markers on IL-17-producing T-cells in PF of endometriosis patients. As shown in Fig. 1A, a substantial PF $CD3^+$ IL-17-producing T-cell population was observed. Further detection revealed that these cells were $CD4^+CXCR3^-$ (Fig. 1B). Based on the expression of CCR6 and CCR4, these cells can be divided into

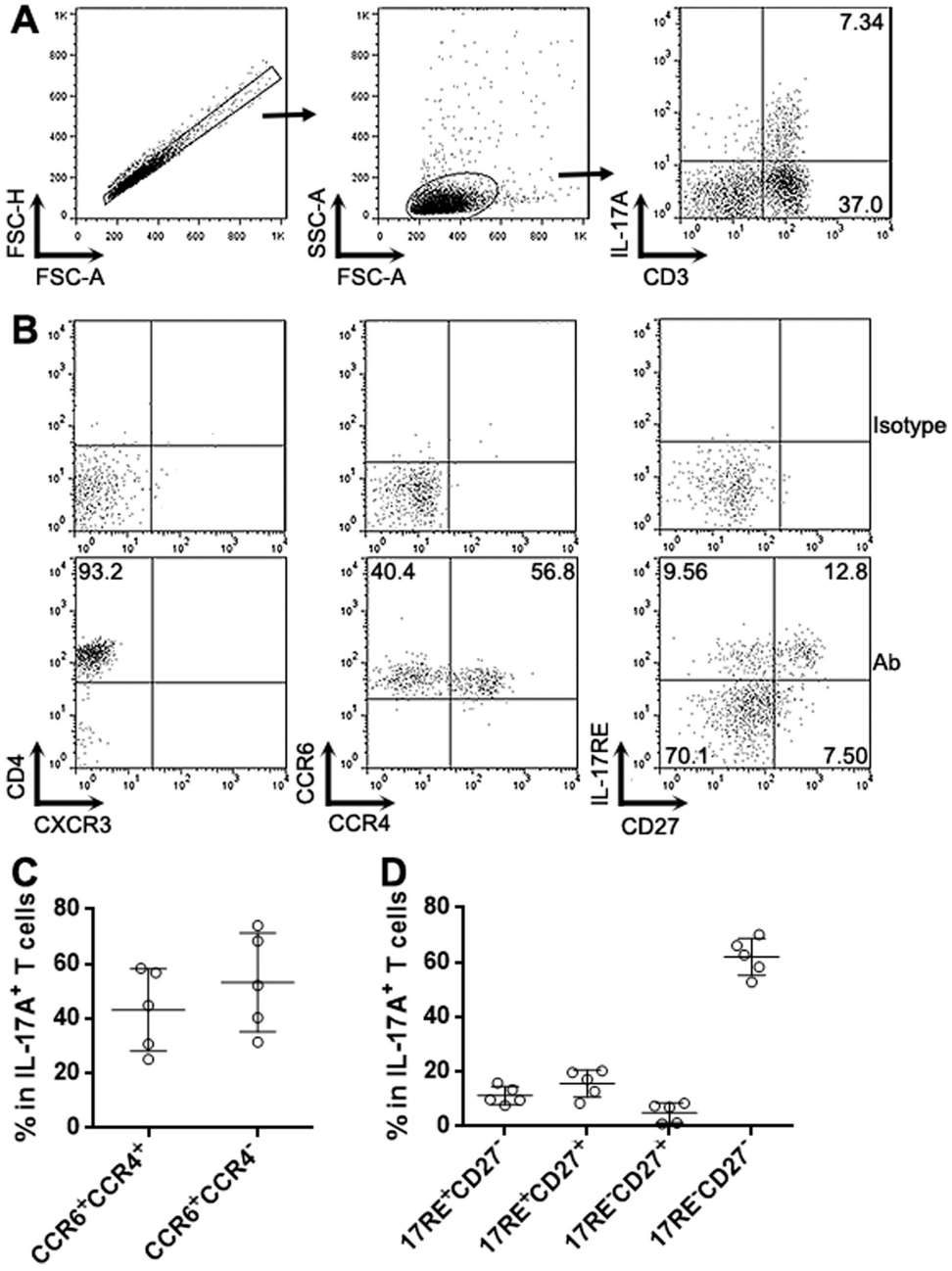

Figure 1. The phenotype of PF IL-17-producing T cells in endometriosis. (A) Representative flow cytometry plots showing IL-17-producing T cells in endometriosis PF. Single cells were gated among the whole events, followed by gating lymphocytes based on FSC-A and SSC-A. $CD3^+IL\text{-}17A^+$ cells were then observed in lymphocytes. Numbers in the quadrants indicate the percentages of cell populations. (B) Detection of indicated surface markers in PF IL-17-producing T cells. Isotype: isotype antibody control. Ab: specific antibody for corresponding markers. (C) Frequencies of $CCR6^+CCR4^+$ and $CCR6^+CCR4^-$ subpopulations in IL-17-producing T cells. (D) Frequencies of $IL\text{-}17RE^+CD27^-$, $IL\text{-}17RE^+CD27^+$, $IL\text{-}17RE^-CD27^+$, and $IL\text{-}17RE^-CD27^-$ subset in IL-17-producing T cells. $N = 5$ individuals per group.

$CCR6^+CCR4^+$ and $CCR6^+CCR4^-$ subpopulations, respectively (Fig. 1B and C). Based on the expression of IL-17RE and CD27, these cells can be divided into $IL\text{-}17RE^+CD27^-$ subset, $IL\text{-}17RE^+CD27^+$ subset, $IL\text{-}17RE^-CD27^+$ subset (very few or almost absent in some samples), and $IL\text{-}17RE^-CD27^-$ subset (Figure 1B and D).

Th17 cells are present in $CCR6^+CCR4^+CXCR3^-CCR10^-$ T-cells

Because IL-17-producing T-cells might involve both Th17 and Th1/17 cells, we needed to accurately discriminate these two populations to isolate live Th17 cells for further investigations. To this end, we analyzed PF $CD3^+CD4^+$ T cells (Fig. 2A) for the expression of CCR6, CCR4, CXCR3, and CCR10. As shown in Fig. 2B, within PF $CD3^+CD4^+$ T cells, four subpopulations were seen based on the expression of CCR4 and CXCR3: $CCR4^+CXCR3^-$ cells, $CCR4^+CXCR3^+$ cells, $CCR4^-CXCR3^+$ cells, and $CCR4^-CXCR3^-$ cells. We then sorted the four subpopulations and measured the expression of T-cell subset master regulators, i.e. T-bet (Gene name TBX21), GATA3, and RORγt. As shown in Fig. 2C, T-bet was highly expressed in $CCR4^-CXCR3^+$ cells while GATA3 was highly expressed in $CCR4^+CXCR3^-$ cells, whereas RORγt was also significantly $CCR4^+CXCR3^-$ cells. This suggested that $CCR4^+CXCR3^-$ cells contained both Th2 and Th17 cells. Interestingly, $CCR4^-CXCR3^+$ T cells, which expressed high T-bet, also expressed moderate levels of RORγt, suggesting that this subpopulation harbored Th1 and Th1/17 cells.

We then dissected $CCR4^+CXCR3^-$ T-cells based on the expression of CCR6 and CCR10. As shown in Fig. 2D, four subpopulations were observed: $CCR6^+CCR10^-$ cells, $CCR6^+CCR10^+$ cells, CCR6-$CCR10^+$ cells, and

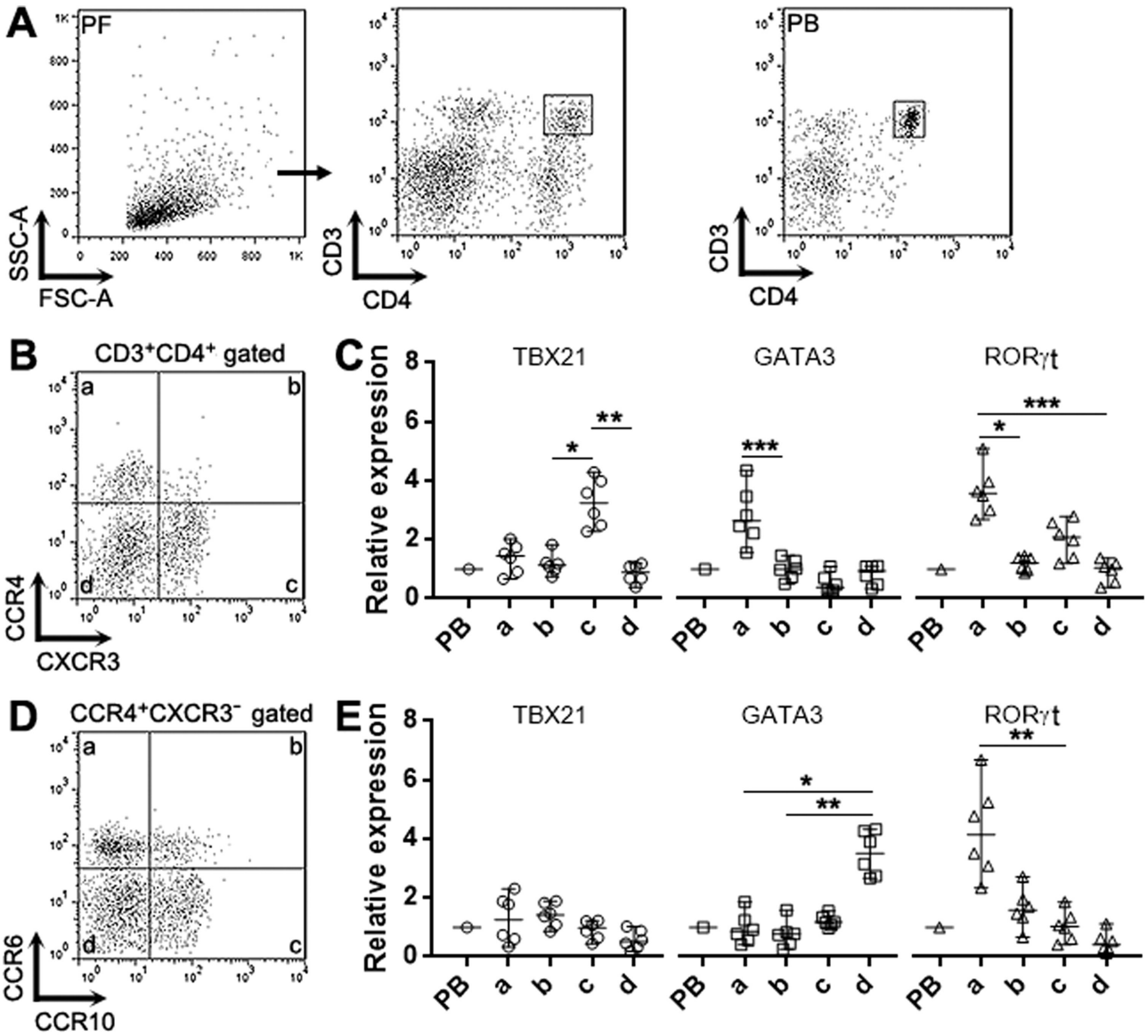

Figure 2. Identification of live PF Th17 cells according to CCR6 and CCR4. (A) Gating of $CD3^+CD4^+$ T cells in endometriosis PF and normal blood. PF: peritoneal fluid. PB: peripheral blood. (B) T cell subsets based on the expression of CCR4 and CXCR3. PB: blood $CD3^+CD4^+$ T cells as control. (C) Relative mRNA levels of indicated master regulators in CCR4-and-CXCR3-defined T cell subsets. (D) Subpopulations in $CCR4^+CXCR3^-$ T-cells based on the expression of CCR6 and CCR10. (E) Relative mRNA levels of indicated master regulators in the subpopulations described in (D). $*P < 0.05$; $**P < 0.01$; $***P < 0.001$. $N = 6$ individuals per group. Kruskal–Wallis test.

CCR6$^-$CCR10$^-$ cells. We then sorted these cells to check the expression of T-bet, GATA3, and RORγt. T-bet expression was ubiquitously low in all four subpopulations, while GATA3 was highly expressed in the CCR6$^-$CCR10$^-$ subpopulation (Fig. 2E). RORγt was robustly expressed in the CCR6$^+$CCR10$^-$ subpopulation but low in the other three subpopulations (Fig. 2E). Therefore, Th17 cells were CCR6$^+$CCR4$^+$CXCR3$^-$CCR10$^-$.

IL-17RE and CD27 expression on live PF Th17 subpopulations

To study live PF Th17 cells, we needed to introduce more fluorophore-conjugated antibodies to label Th17 cells. However, it is difficult for conventional flow cytometers without ultraviolet lasers to recognize more than 6 fluorophores. Therefore, we came up with a new method to distinguish live Th17 cells. PE-conjugated anti-CD14 antibody, anti-CXCR3 antibody, and anti-CCR10 antibody were used together to exclude CD14$^+$ macrophages, CXCR3$^+$ Th1 cells, CXCR3$^+$ Th1/17 cells, and other non-Th2 and non-Th17 T-cells (Fig. 3A). Within the CD14$^-$CXCR3$^-$CCR10$^-$ cells, CD4$^+$ T-cells were divided into four subpopulations according to the expression of CCR6 and CCR4: CCR6$^+$CCR4$^-$ cells, CCR6$^+$CCR4$^+$ cells, CCR6$^-$CCR4$^+$ cells, and CCR6$^+$CCR4$^+$ cells (Fig. 3A). Evaluation of T-cell subset master regulators indicated that RORγt was exclusively highly expressed in the CCR6$^+$CCR4$^+$ subpopulation while GATA3 was predominantly expressed in the CCR6$^-$CCR4$^+$ subpopulation (Fig. 3B). Consistently, analysis of IL-17A expression confirmed that the CCR6$^+$CCR4$^+$ subpopulation was Th17 cells (Fig. 3C and D). Previous studies have reported the significance of IL-17RE and CD27 to Th17 activity [14, 15]. Therefore, we further dissected the CCR6$^+$CCR4$^+$ subpopulation based on the expression of IL-17RE and CD27. As shown in Fig. 3E, the CCR6$^+$CCR4$^+$ subpopulation was divided into three subsets: IL-17RE$^+$CD27$^-$ cells, IL-17RE$^+$CD27$^+$ cells, and IL-17RE$^-$CD27$^-$ cells. The IL-17RE$^+$CD27$^-$ subset and IL-17RE$^+$CD27$^+$ subset expressed higher IL-17A than the IL-17RE$^-$CD27$^-$ subset (Fig. 3F). However, their RORγt expression was comparable (Fig. 3G). Therefore, IL-17RE and CD27 signify the heterogeneity of PF Th17 cells.

PF IL-17RE$^+$ Th17 cells are more pro-inflammatory than IL-17RE$^-$ Th17 cells

Assessment of the expression of other Th17-related cytokines indicated that in comparison with the IL-17RE$^-$CD27$^-$ subset,

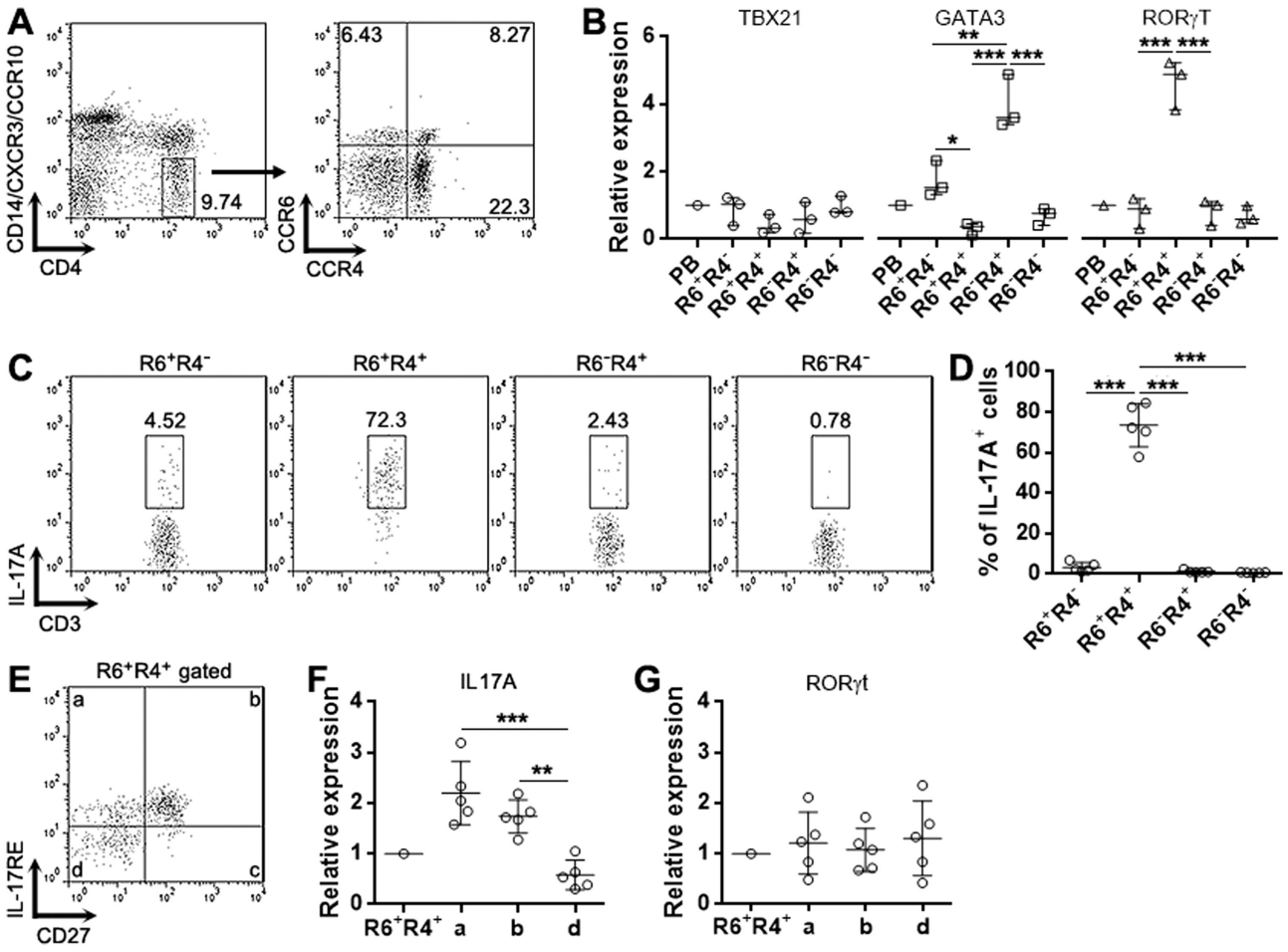

Figure 3. Identification of live PF Th17 subsets according to IL-17RE and CD27. (A) Subsets in CD14$^-$CXCR3$^-$CCR10$^-$CD4$^+$ cells based on the expression of CCR6 and CCR4. (B) Relative mRNA levels of indicated master regulators in the subpopulations described in (A). PB: blood CD3$^+$CD4$^+$ T cells as control. R6: CCR6. R4: CCR4. $N = 3$ per group. (C) Flow cytometry plots showing IL-17A expression in the subpopulations described in (A). (D) Frequencies of IL-17A$^+$ cells in the 4 subpopulations. (E) Expression of IL-17RE and CD27 on the surface of the CCR6$^+$CCR4$^+$ subpopulation. (F) Relative mRNA levels of IL-17A in IL-17RE$^+$CD27$^-$ cells, IL-17RE$^+$CD27$^+$ cells, and IL-17RE-CD27$^-$ cells. (G) Relative mRNA levels of RORγt in the same three subsets as (F). $^*P < 0.05$; $^{**}P < 0.01$; $^{***}P < 0.001$. $N = 5$ per group in (D) to (G). Kruskal–Wallis test.

the IL-17RE$^+$CD27$^-$ subset and IL-17RE$^+$CD27$^+$ subset produced more GM-CSF (Fig. 4A and B) as well as IL-22 mRNA (Fig. 4C). Furthermore, evaluation of cell cycle using Hoechst 33342 and Pyronin Y demonstrated that the IL-17RE$^+$CD27$^-$ subset and IL-17RE$^+$CD27$^+$ subset had more cells in the G1 phase and S-G2/M phase than the IL-17RE$^-$CD27$^-$ subset, suggesting that the former two subsets were more proliferative than the latter (Fig. 4D). Therefore, IL-17RE$^+$ Th17 cells were more pro-inflammatory than IL-17RE$^-$ Th17 cells. CD27 did not profoundly influence Th17 activity because no significant difference was seen between the IL-17RE$^+$CD27$^-$ subset and IL-17RE$^+$CD27$^+$ subset. In addition, we compared the frequencies of IL-17RE$^+$ Th17 cells and IL-17RE$^-$ Th17 cells in PF CCR6$^+$CCR4$^+$ T cells enriched from patients with stage III endometriosis and patients with stage IV endometriosis. It turned out that no significant difference was observed (Fig. S1).

To characterize blood Th17 subsets, blood leukocytes were subjected to the same staining and detection protocol. As shown in Fig. S2, the CCR6$^+$CCR4$^+$ population accounted for less than 3% of CD14$^-$CXCR3$^-$CCR10$^-$CD4$^+$ T cells, while the IL-17RE$^+$ subset accounted for less than 5% of the CCR6$^+$CCR4$^+$ population. Therefore, Th17 cells and their subpopulations were rare in circulating T cells. Due to this rarity, we mainly focused on PF Th17 cells in the following experiments.

PF IL-17RE$^+$Th17 cells and IL-17RE$^-$Th17 cells have distinct gene expression profiles

To deeply understand the molecular traits of PF IL-17RE$^+$ Th17 cells and IL-17RE$^-$ Th17 cells, we sorted these cells to conduct the RNA-Seq analysis (Fig. 5A). Compared with IL-17RE$^-$ Th17 cells, a total of 5288 differentially expressed

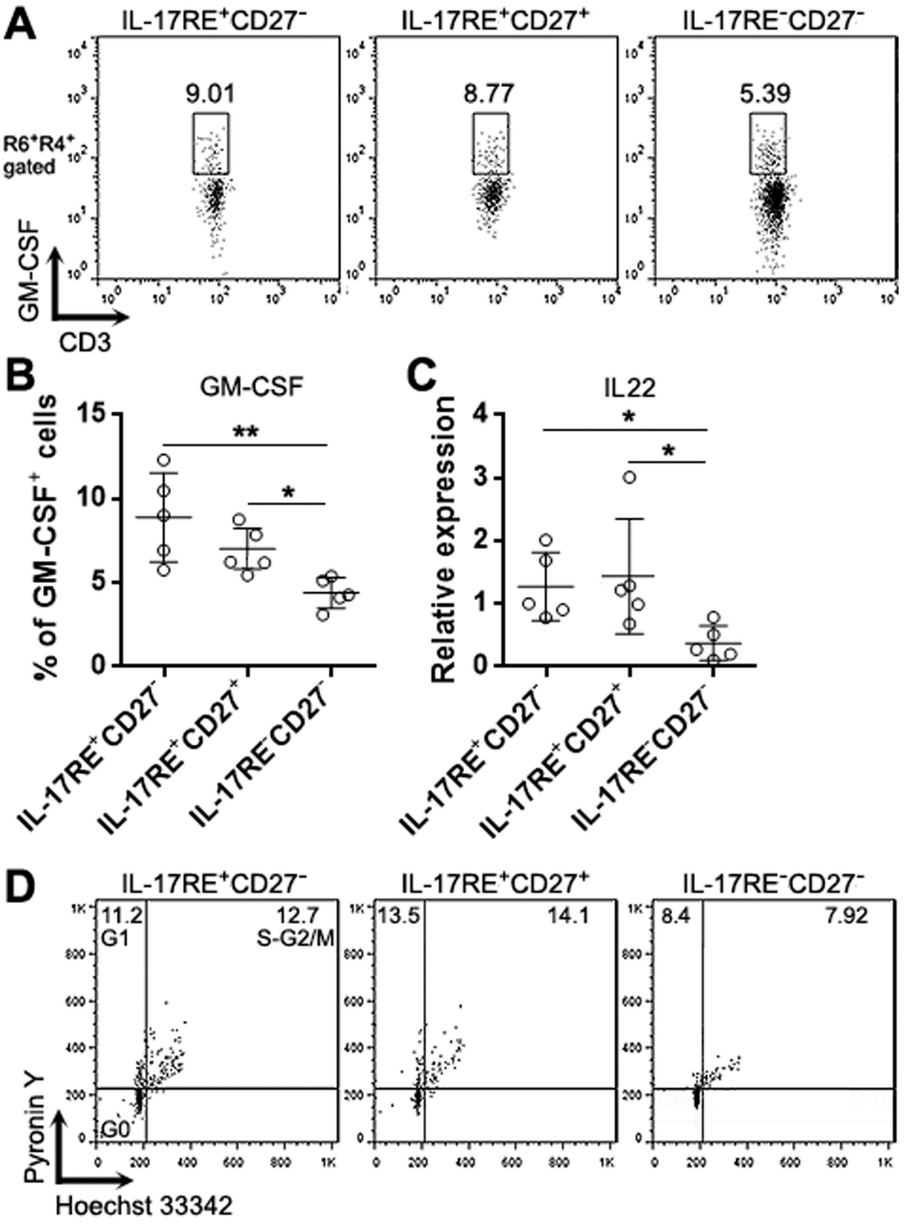

Figure 4. Functions of PF Th17 subsets. (A & B) GM–CSF expression in IL-17RE$^+$CD27$^-$ subset, IL-17RE$^+$CD27$^+$ subset, and IL-17RE$^-$CD27$^-$ subset. Representative flow cytometry plots are shown in (A), and statistics of the frequencies of GM–CSF$^+$ cells are shown in (B). (C) Relative mRNA levels of IL22 in the three subsets. $N = 5$ per group. Kruskal–Wallis test. (D) Flow cytometry plots showing cell cycle measured by staining with Hoechst 33342 and Pyronin Y. $*P < 0.05$; $**P < 0.01$.

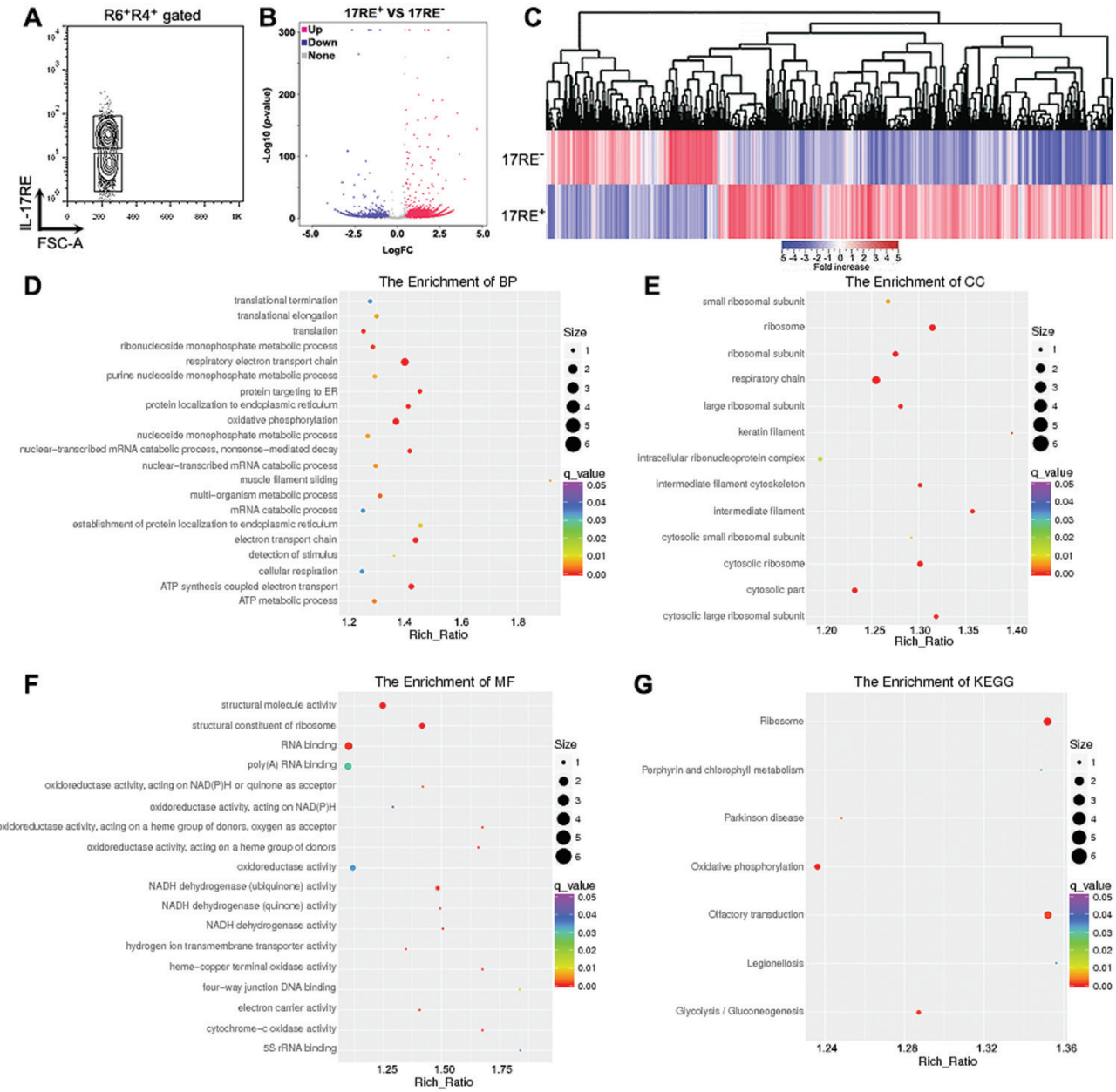

Figure 5. RNA-Seq analysis of PF IL-17RE$^+$ Th17 cells and IL-17RE$^-$ Th17 cells. (A) Gating and sorting of PF CCR6$^+$CCR4$^+$IL-17RE$^+$ Th17 cells and CCR6$^+$CCR4$^+$IL-17RE$^-$ Th17 cells. (B) Volcano plot displaying the DETs. (C) Cluster analysis of DETs. 17RE$^-$: IL-17RE$^-$ Th17. 17RE$^+$: IL-17RE$^+$ Th17. (D–F) Enrichment of up-regulated DETs for GO terms in the category of biological process terms (D), cellular component terms (E), and molecular function terms (F). (G) Enrichment of up-regulated DETs for KEGG terms.

transcripts (DETs) were identified in IL-17RE$^+$ Th17 cells, including 3866 up-regulated DETs and 1422 down-regulated DETs (Fig. 5B and C). The GO biological process (BP) enrichment results showed significant associations with respiratory electron transport chain, oxidative phosphorylation, and ATP synthesis coupled transport, etc. (Fig. 5D). GO cellular component (CC) analysis showed notable associations with respiratory chain, ribosome, and ribosomal subunit, etc. (Fig. 5E). GO molecular function (MF) analysis showed remarkable associations with structural molecular activity, structural constituent of ribosome, RNA binding, NADH dehydrogenase (ubiquinone) activity, and other metabolism-related activity (Fig. 5F). KEGG analysis also enriched DETs in certain KEGG terms such as the ribosome, oxidative phosphorylation, olfactory transduction, and glycolysis/gluconeogenesis (Fig. 5G). Hence, the expression of genes for OXPHOS and ETC seemed to be remarkably increased in IL-17RE$^+$ Th17 cells relative to IL-17RE$^-$ Th17 cells.

IL-17RE$^+$Th17 cells generate more ATP and ROS

Analysis of metabolism-related DETs revealed that in comparison to PF IL-17RE$^-$ Th17 cells, PF IL-17RE$^+$ Th17 cells up-regulated the expression of genes involved in OXPHOS and ETC, including *NDUFB5*, *MT-CO1*, *UQCRC1*, and *NDUFS6*, etc. (Fig. 6A and Table 2). The up-regulation of these genes was validated by qRT-PCR (Fig. 6B). Since OXPHOS and ETC are crucial for the generation of ATP and ROS, we quantified ATP and ROS in the two Th17 subsets.

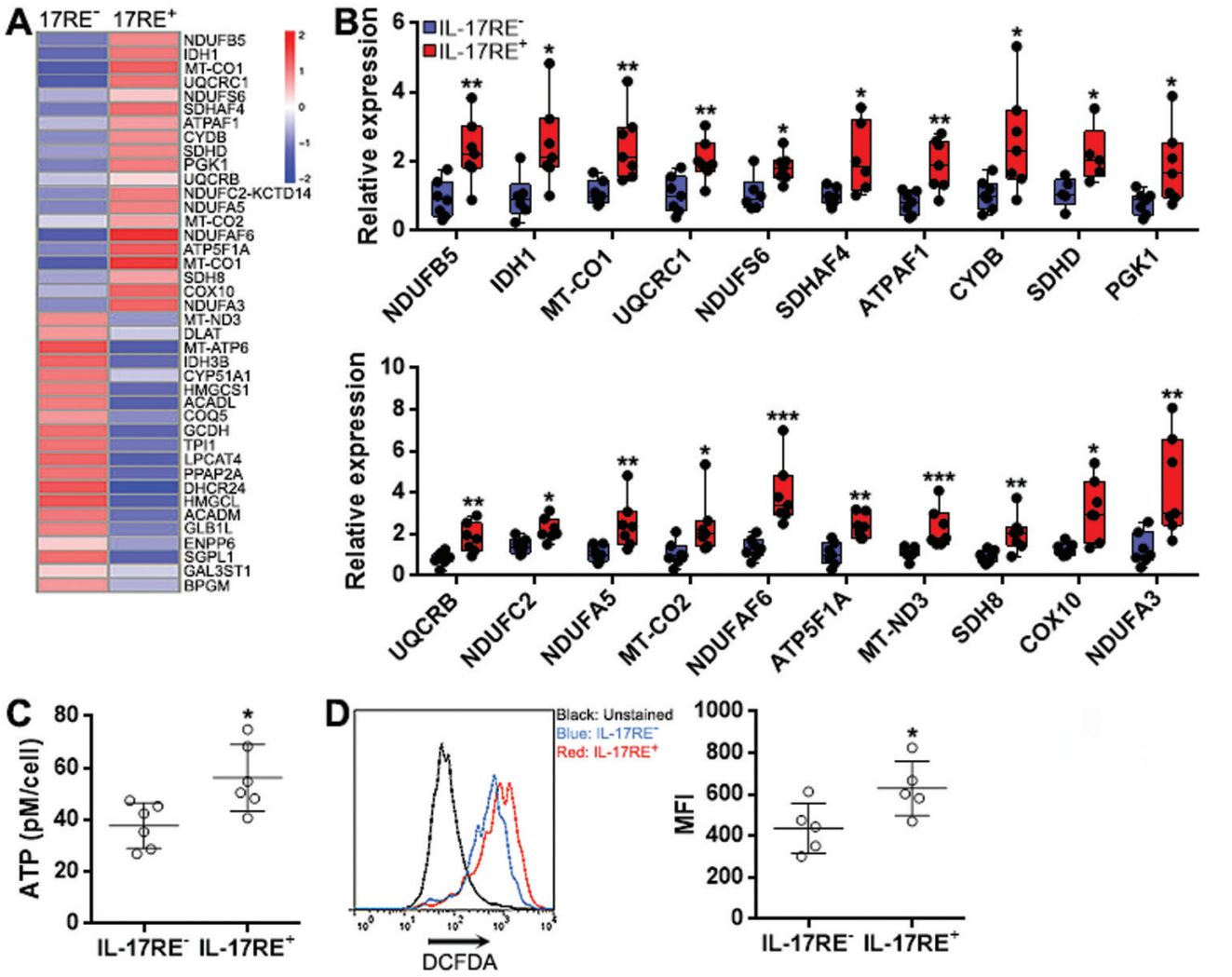

Figure 6. OXPHOS and ETC in PF IL-17RE$^+$ Th17 cells and IL-17RE$^-$ Th17 cells. (A) Heat map of top 40 metabolism-related DETs (FDR < 0.05). (B) Validation of DETs in (A) by qRT-PCR. N = 5–7 per group. The data are presented as min to max. (C) ATP levels in IL-17RE$^+$ Th17 cells and IL-17RE$^-$ Th17 cells. N = 6 per group. (D) ROS levels measured by H2DCFDA staining. N = 5 per group. $^*P < 0.05$; $^{**}P < 0.01$; $^{***}P < 0.001$. Mann–Whitney U test.

As shown in Fig. 6C, IL-17RE$^+$ Th17 cells produced more ATP than IL-17RE$^-$ Th17 cells. H2DCFDA staining suggested more ROS generation in IL-17RE$^+$ Th17 cells relative to IL-17RE$^-$ Th17 cells (Fig. 6D). The top 20 down-regulated metabolic genes were largely associated with other metabolic pathways (Table 3). Therefore, IL-17RE$^+$ Th17 cells and IL-17RE$^-$ Th17 cells are metabolically different. Furthermore, the expression of the above-mentioned up-regulated metabolic genes in IL-17RE$^+$ Th17 cells was comparable between stage III endometriosis and stage IV endometriosis (Fig. S3). Therefore, the OXPHOS-and-ETC-associate gene expression profiles did not correlate to disease severity. Additionally, no significant correlation between PF ROS level and endometriosis stage was found (Fig. S4).

Discussion

In the current study, we developed a method to sort live Th17 cells from PF of severe endometriosis patients to evaluate the function of pathological Th17 cells. We are the first to use CXCR3, CCR4, and CCR6 to isolate PF Th17 cells from endometriosis patients. In the future, it would be necessary to detect more surface markers to precisely pinpoint Th17 cells. Furthermore, the above chemokine receptors would greatly facilitate T cell research in endometriosis.

Th17 cells are heterogeneous and possess a remarkable degree of plasticity [16]. Our study indicates that PF Th17 cells are heterogeneous according to the expression of CD27 and IL-17RE. CD27 is a member of the TNF receptor family expressed on CD4$^+$ T cells at the priming or effector stage, while its ligand, CD70, is expressed on activated dendritic cells and lymphocytes [17]. Recent research suggests its inhibitory effect on Th17 cells through repressing transcription of IL-17 and CCR6 [15]. IL-17RE forms a receptor complex with IL-17RA to bind to IL-17C to potentiate the Th17 cell response [14]. IL-17C is preferentially secreted by epithelial cells in the lung, skin, and colon [18]. Interestingly, the Human Protein Atlas describes high IL-17C expression in the endometrium (https://www.proteinatlas.org/ENSG00000124391-IL17C/tissue), strongly suggesting the existence of IL-17C in endometriosis lesions. Our ongoing research is investigating the levels of IL-17C in PF and endometriosis tissues. Besides, our data indicate that IL-17RE rather than CD27 marks a more active Th17 subpopulation,

Table 2. Twenty up-regulated metabolic genes in IL-17RE$^+$ Th17 cells

Gene	Protein
MT-ND3	NADH-ubiquinone oxidoreductase chain 3
DLAT	Dihydrolipoyllysine-residue acetyltransferase component of pyruvate dehydrogenase complex
MT-ATP6	F-ATPase protein 6
IDH3B	Isocitrate dehydrogenase [NAD] subunit beta
CYP51A1	Lanosterol 14-alpha demethylase
HMGCS1	Hydroxymethylglutaryl-CoA synthase, cytoplasmic
ACADL	Long-chain specific acyl-CoA dehydrogenase
COQ5	2-methoxy-6-polyprenyl-1,4-benzoquinol methylase
GCDH	Glutaryl-CoA dehydrogenase
TPI1	Triosephosphate isomerase
LPCAT4	Lysophospholipid acyltransferase
PPAP2A	Lipid phosphate phosphohydrolase 1
DHCR24	Delta(24)-sterol reductase
HMGCL	Hydroxymethylglutaryl-CoA lyase
ACADM	Medium-chain specific acyl-CoA dehydrogenase
GLB1L	Beta-galactosidase-1-like protein
ENPP6	Glycerophosphocholine cholinephosphodiesterase
SGPL1	Sphingosine-1-phosphate lyase 1
GAL3ST1	Galactosylceramide sulfotransferase
BPGM	Bisphosphoglycerate mutase

Table 3. Twenty down-regulated metabolic genes in IL-17RE$^+$ Th17 cells

Gene	Protein
NDUFB5	NADH dehydrogenase [ubiquinone] 1 beta subcomplex subunit 5
IDH1	Isocitrate dehydrogenase [NADP+] Cytoplasmic
MT-CO1	Cytochrome c oxidase subunit 1
UQCRC1	Cytochrome b-c1 complex subunit 1
NDUFS6	NADH dehydrogenase [ubiquinone] iron-sulfur protein 6
SDHAF4	Succinate dehydrogenase assembly factor 4
ATPAF1	ATP synthase mitochondrial F1 complex assembly factor 1
CYDB	Cytochrome bd-I ubiquinol oxidase subunit 2
SDHD	Succinate dehydrogenase [ubiquinone] cytochrome b small subunit
PGK1	Phosphoglycerate kinase 1
UQCRB	Cytochrome b-c1 complex subunit 7
NDUFC2	NADH dehydrogenase [ubiquinone] 1 subunit C2
NDUFA5	NADH dehydrogenase [ubiquinone] 1 alpha subcomplex subunit 5
MT-CO2	Cytochrome c oxidase subunit 2
NDUFAF6	NADH dehydrogenase [ubiquinone] complex I, assembly factor 6
ATPAF1A	ATP synthase mitochondrial F1 complex assembly factor 1
MT-ND3	NADH-ubiquinone oxidoreductase chain 3
SDH8	Succinate dehydrogenase assembly factor 4
COX10	Protoheme IX farnesyltransferase
NDUFA3	NADH dehydrogenase [ubiquinone] 1 alpha subcomplex subunit 3

because IL-17RE$^+$ Th17 cells expressed more Th17-related cytokines and were more proliferative. A possible explanation is that IL-17RE-triggered signaling overcomes CD27-induced signaling.

Through RNA-Seq, we found that most of the top 20 up-regulated metabolic genes in IL-17RE$^+$ Th17 cells encode enzymes involved in OXPHOS and ETC, while most of the down-regulated metabolic genes were associated with other metabolic pathways. Mitochondrial respiration is enhanced during Th17 differentiation and OXPHOS is essential for Th17 cell pathogenic signature gene expression [19]. Besides, Th17 cells have limited capacity to promote glycolysis to react to metabolic stresses and they rely on OXPHOS to produce energy and cytokines [20]. Indeed, we observed higher pro-inflammatory activity associated with more ATP and ROS in IL-17RE$^+$ Th17 cells. This suggests that OXPHOS and ETC support the pathogenicity of PF IL-17RE$^+$ Th17 cells in endometriosis. Our data also poses an interesting question: whether the IL-17C/IL-17RE axis results in the up-regulation of OXPHOS and ETC-related genes. This could be answered in future studies.

What remains unknown is the origin of the heterogeneous PF Th17 subsets. Are they a CD4$^+$ T cell population at different maturation statuses? Or do they arise from different CD4$^+$ T cell subsets under distinct microenvironment factors? Lineage tracing of Th17 cells in animal models and single-cell transcriptome sequencing might answer these questions.

In conclusion, this study provides a novel method to detect and isolate live PF Th17 cells from endometriosis patients and unveils the functional and metabolic heterogeneity of PF Th17 subsets. Furthermore, the data of other differentially expressed genes shed light on the elucidation of molecular mechanisms underlying the function of pathological Th17 cells.

Supplementary data

Supplementary data is available at *Clinical and Experimental Immunology* online.

Supplementary Table1: Primer sequences

Supplementary Figure 1: The frequencies of IL-17RE$^+$ Th17 cells and IL-17RE$^-$ Th17 cells in PF CCR6$^+$CCR4$^+$ T cells enriched from patients with stage III endometriosis (III) and patients with stage IV endometriosis (IV). N = 6 individuals per group. Mann–Whitney U test.

Supplementary Figure 2: IL-17RE$^+$ Th17 cells and IL-17RE$^-$ Th17 cells in peripheral blood. (A) Representative flow cytometry plots showing blood Th17 subsets. CD14$^-$CXCR3$^-$CCR10$^-$CD4$^+$ T cells were first gated, followed by gating CCR6$^+$CCR4$^+$ T cells. Th17 subsets were then distinguished based on the expression of IL-17RE and CD27. (B) Statistics of the frequencies of IL-17RE$^+$ Th17 cells and IL-17RE$^-$ Th17 cells in blood CCR6$^+$CCR4$^+$ T cells. III: patients with stage III endometriosis. IV: patients with stage IV endometriosis. N = 5 per group.

Supplementary Figure 3: Relative expression of indicated metabolic genes in IL-17RE$^+$ Th17 cells sorted from patients with stage III endometriosis (III) and patients with stage IV endometriosis (IV). N = 6 individuals per group. Mann-Whitney U test.

Supplementary Figure 4: ROS levels in PF of patients with stage III endometriosis (III) and patients with stage

IV endometriosis (IV). $N = 6$ individuals per group. Mann-Whitney U test.

Acknowledgements

None

Funding

There are no funders to report for this submission.

Conflicts of interest

The authors declare no conflict of interest.

Author contributions

Y.J. Performed the experiment and the data analyses, and wrote the manuscript. L.W. Performed the experiment and wrote the manuscript. Y.J., L.W. Contributed equally to this work and should be considered co-first authors. Y.P. Contributed significantly to analysis and manuscript preparation. J.Q. Contributed to the conception of the study. A.T. Helped perform the analysis with constructive discussions. S.W. Helped perform data analyses.

References

1. Chapron C, Marcellin L, Borghese B, Santulli P. Rethinking mechanisms, diagnosis and management of endometriosis. *Nat Rev Endocrinol* 2019, 15, 666–82.
2. Vallvé-Juanico J, Houshdaran S, Giudice LC. The endometrial immune environment of women with endometriosis. *Hum Reprod Update* 2019, 25, 564–91.
3. Izumi G, Koga K, Takamura M, Makabe T, Satake E, Takeuchi A, et al. Involvement of immune cells in the pathogenesis of endometriosis. *J Obstet Gynaecol Res* 2018, 44, 191–8.
4. Szyllo K, Tchorzewski H, Banasik M, Glowacka E, Lewkowicz P, Kamer-Bartosinska A. The involvement of T lymphocytes in the pathogenesis of endometriotic tissues overgrowth in women with endometriosis. *Mediators Inflamm* 2003, 12, 131–8.
5. Tanaka Y, Mori T, Ito F, Koshiba A, Takaoka O, Kataoka H, et al. Exacerbation of Endometriosis due to regulatory T-cell dysfunction. *J Clin Endocrinol Metab* 2017, 102, 3206–17.
6. Takamura M, Koga K, Izumi G, Hirata T, Harada M, Hirota Y, et al. Simultaneous detection and evaluation of four subsets of CD4+ T lymphocyte in lesions and peripheral blood in endometriosis. *Am J Reprod Immunol* 2015, 74, 480–6.
7. Gogacz M, Winkler I, Bojarska-Junak A, Tabarkiewicz J, Semczuk A, Rechberger T, et al. Increased percentage of Th17 cells in peritoneal fluid is associated with severity of endometriosis. *J Reprod Immunol* 2016, 117, 39–44.
8. Zhao F, Hoechst B, Gamrekelashvili J, Ormandy LA, Voigtländer T, Wedemeyer H, et al. Human CCR4+ CCR6+ Th17 cells suppress autologous CD8+ T cell responses. *J Immunol* 2012, 188, 6055–62.
9. Halim L, Romano M, McGregor R, Correa I, Pavlidis P, Grageda N, et al. An atlas of human regulatory T helper-like cells reveals features of Th2-like tregs that support a tumorigenic environment. *Cell Rep* 2017, 20, 757–70.
10. Pandya JM, Lundell AC, Hallström M, Andersson K, Nordström I, Rudin A. Circulating T helper and T regulatory subsets in untreated early rheumatoid arthritis and healthy control subjects. *J Leukoc Biol* 2016, 100, 823–33.
11. Gosselin A, Monteiro P, Chomont N, Diaz-Griffero F, Said EA, Fonseca S, et al. Peripheral blood CCR4+CCR6+ and CXCR3+CCR6+CD4+ T cells are highly permissive to HIV-1 infection. *J Immunol* 2010, 184, 1604–16.
12. Mony JT, Khorooshi R, Owens T. Chemokine receptor expression by inflammatory T cells in EAE. *Front Cell Neurosci* 2014, 8, 187.
13. Wang C, Kang SG, Lee J, Sun Z, Kim CH. The roles of CCR6 in migration of Th17 cells and regulation of effector T-cell balance in the gut. *Mucosal Immunol* 2009, 2, 173–83.
14. Chang SH, Reynolds JM, Pappu BP, Chen G, Martinez GJ, Dong C. Interleukin-17C promotes Th17 cell responses and autoimmune disease via interleukin-17 receptor E. *Immunity* 2011, 35, 611–21.
15. Coquet JM, Middendorp S, van der Horst G, Kind J, Veraar EA, Xiao Y, et al. The CD27 and CD70 costimulatory pathway inhibits effector function of T helper 17 cells and attenuates associated autoimmunity. *Immunity* 2013, 38, 53–65.
16. Bystrom J, Clanchy FIL, Taher TE, Al-Bogami M, Ong VH, Abraham DJ, et al. Functional and phenotypic heterogeneity of Th17 cells in health and disease. *Eur J Clin Invest* 2019, 49, e13032.
17. Borst J, Hendriks J, Xiao Y. CD27 and CD70 in T cell and B cell activation. *Curr Opin Immunol* 2005, 17, 275–81.
18. Nies JF, Panzer U. IL-17C/IL-17RE: emergence of a unique axis in TH17 biology. *Front Immunol* 2020, 11, 341.
19. Shin B, Benavides GA, Geng J, Koralov SB, Hu H, Darley-Usmar VM, et al. Mitochondrial oxidative phosphorylation regulates the fate decision between pathogenic Th17 and regulatory T cells. *Cell Rep* 2020, 30, 1898–1909.e4.
20. Franchi L, Monteleone I, Hao LY, Spahr MA, Zhao W, Liu X, et al. Inhibiting oxidative phosphorylation in vivo restrains Th17 effector responses and ameliorates murine colitis. *J Immunol* 2017, 198, 2735–46.